

X-ray Measurements of Black Hole X-ray Binary Source GRS 1915+105 and the Evolution of Hard X-ray Spectrum

R. K. Manchanda, *Tata Institute of Fundamental Research, Mumbai 400005, India.*

Received 1999 December 28; accepted 2000 February 9

Abstract. We report the spectral measurement of GRS 1915+105 in the hard X-ray energy band of 20–140keV. The observations were made on March 30th, 1997 during a quiescent phase of the source. We discuss the mechanism of emission of hard X-ray photons and the evolution of the spectrum by comparing the data with earlier measurements and an axiomatic model for the X-ray source.

Key words. Accretion, accretion disks—X-rays: stars—Black hole candidates, binary sources: individual—GRS 1915+105.

1. Introduction

Since its discovery in 1992 (Castro-Tirado *et al.* 1992), the Galactic X-ray transient source GRS 1915+105 has exhibited pronounced active phases during 1994, 1996 and 1997. A long term temporal behaviour of the source suggests an abundant mixture of outbursts and low luminosity episodes. The variety of other short term temporal features in the X-ray light curve include flickering, strong quasi-periodic oscillations, irregular X-ray bursts, pronounced dips and rapid high-low transitions both in soft and hard X-ray bands (Greiner *et al.* 1996; Morgan *et al.* 1997; Yadav *et al.* 1999).

Among the main dynamical features of the source are the emission of two symmetric radio jets with superluminal motion (Mirabel & Rodriguez 1994), super Eddington X-ray luminosity of 6.5×10^{39} erg/sec in the 6–120 keV band (Greiner *et al.* 1998) on various occasions and the presence of strong 0.5–10 Hz QPOs apart from the two spectral states signifying the ‘High’ and ‘Low’ state (Trudolyubov *et al.* 1998). GRS 1915+105 is one of the two known Galactic sources that exhibit superluminal radio jets (Mirabel & Rodriguez 1994). From the radio measurements in the H_r band and the relativistic constraints on the superluminal motion, the distance of the source is estimated to be 12.5 ± 1.5 kpc. A probable counterpart with 23.4 mag in I band has been claimed to be detected by Mirabel *et al.* (1994) and recently a 52^d orbital period has been proposed from the analysis of the RXTE and BATSE light curves (Manchanda 1999). In the absence of a definite optical identification of the primary component, the true nature of the source is still unresolved.

Simultaneous observations of the source in radio, IR and X-ray band indicate a synchrotron origin of the low energy photons instead of thermal reprocessing of the X-rays (Foster *et al.* 1996; Fender *et al.* 1997). While the X-ray and Infrared photons show a one-to-one correlation, the time offset and the shape comparison suggest the decoupling between the two during the later stage (Eikenberry *et al.* 1998).

The X-ray luminosity from the source is observed to rise to super Eddington limit on several occasions, thereby suggesting the black-hole nature of the underlying object. Furthermore, on the basis of phenomenological arguments of similarity of two X-ray spectral states ‘high soft’ and ‘low hard’ to the well known BH candidates, absence of pulsation, correlation of the QPO power with the high spectral state, GRS 1915+105 is believed to be a black hole candidate. In addition, the temporal profile of the X-ray burst of slow rise and rapid decay and the hardening of the X-ray spectrum within the burst is taken to be the evidence of disappearance of the inner accretion disk into black-hole horizon (Belloni *et al.* 1997a). A variety of theoretical models involving bulk-motion, advection driven accretion and multi-colour black body emission have been invoked to explain the spectral and temporal features of the source. The periods of weaker emission, outburst and rapid flaring are believed to be due to rapid removal and replenishment of the inner part of the accretion disk (Belloni *et al.* 1997b), the X-ray spectrum is believed to originate by Compton upgradation of the keV photons (Titarchuk & Zannias 1998).

The evolution of the hard X-ray spectrum of GRS 1915+105 and its relation to the 1–10 keV flux does not indicate any well defined correlation. However, in general the low energy data below 30keV on the transient galactic black hole candidates suggest the presence of at least two main spectral states apart from the quiescent emission during which $L_x < 10^{-4}L_{\text{Edd}}$ which are distinguished by the amount of soft 1–10 keV and ultra soft X-ray photons while the hard X-ray spectrum above 30 keV, in the two states are characterized by a power law tail with spectral index $\alpha \sim 2 - 3$ during high state and the $\alpha \sim 1.5 - 2$ during the low state.

In this paper we present the spectral measurement of GRS 1915+105 in the hard X-ray region made during the post-burst quiescent state. We discuss the spectral evolution using the RXTE measurements of the source made before and after our observations.

2. Instrument and observation

The observations were made with a Large Area Scintillation counter Experiment (LASE) which is designed to study fast variations in the flux of X-ray sources in the hard X-ray energy region up to 200 keV. The payload consists of three large area X-ray detector modules mounted on a servo-controlled platform. The detectors are a specially designed combination of thin and thick large area NaI(Tl) scintillation counters configured in back-to-back geometry. Each of the detector modules has a geometrical area of 400 cm² and the thickness of the prime detector is 3 mm. The active anti-coincidence shield is provided by a 30 mm thick crystal. The field of view of each module is 4.5°×4.5° and is defined by demountable mechanical slat collimator specially designed with a sandwiched material of lead, tin and copper. Each module along with the collimator is further encased with a passive shield. Each detector is designed as a stand-alone unit with independent on-board subsystems for HV power and data processing. The payload platform is servo-stabilized and the target X-ray source and the corresponding background region are tracked using an on-board micro-processor controlled tracker.

The detectors have almost 100% detection efficiency in the operative energy range and the back-to-back configuration gives 80% reduction in the detector background,

most of which is produced due to partial energy loss by the Compton scattering of high energy photons in the main detector. The preflight calibration of the X-ray detectors is done at different energies using radioactive sources, Cd¹⁰⁹ (22.1, 87.5 keV), Am²⁴¹ (24.7 and 59.6keV) and Ba¹³³ (32.4 and 81keV). In addition, an Am²⁴¹ source is mounted on the pay load for the calibration of the detectors during the flight using ground command. The accepted events are pulse-height analyzed, time tagged with a 25 μ sec resolution and transmitted to ground on a 40 Kbit PCM/FM link. The details of the detector design, associated electronics, control sub-systems and in-flight behaviour of the instrument are presented elsewhere (D'Silva *et al.* 1998). A 3 σ sensitivity of the LASE telescope in the entire energy range up to 180keV is $\sim 1.5 \times 10^{-6} \text{cm}^{-2} \text{s}^{-1} \text{keV}^{-1}$ for a source observation of 10⁴ sec.

The balloon flight was launched on March 30th, 1997 from Hyderabad, India (cut-off rigidity 16.8 GV) and reached the ceiling altitude of 3.3 mbars. A number of X-ray sources in the right ascension band of 16^h to 22^h were observed during the experiment. GRS 1915+105 was in the field of view of two detectors for a total period of 60 min (two sightings of 30 min each) between 0235 UT and 0350 UT and the background was measured for 20 min each before and after the source observation and for 10 min midway the source pointings. The off-source pointing location was carefully selected blank field from the known X-ray source catalog. The X-ray light curve from the all sky monitor on-board RXTE, suggests that at the time of our observation the source was in a post burst quiescent phase with source luminosity twice the lowest value.

3. Results and discussion

A total excess of 10300 counts due to GRS 1915+105 were recorded in the two detectors. This corresponds to a combined statistical significance of 20 σ . The positive excess was seen up to 140 keV. The source contribution was divided in 10 energy bins and corrected for atmospheric absorption, window transmission, detector efficiency and energy resolution for each detector and co-added. The combined spectrum of the source is shown in Fig. 1. The errors on the data points correspond to 1 σ statistical errors. A systematic error of $\sim 10\%$ is estimated for the lowest energy channel and included in the plot. For comparison, we have also plotted the hard X-ray spectrum of the well known BH candidate Cyg X-1 during the 'low hard' X-ray state, shown with dotted line in the figure.

A single power law fit of the form $dN/dE = KE^{-\alpha}$ photons $\text{cm}^{-2} \text{s}^{-1} \text{keV}^{-1}$ to the spectral data gives the best fit model parameters of $K = 36.8 \pm 2.6$ and $\alpha = 3.34 \pm 0.25$ for a χ^2 value of 0.31 per dof. The solid line in the figure shows the fitted spectrum. A simple comparison with the earlier data is not possible because the only composite model fits for the soft and hard X-ray band are used and the best fit parameters are quoted for the individual components. The spectral fits in the low energy domain are more complex as even in the simplest models, multi-colour temperature, equivalent hydrogen column density and contribution due to iron-line features are the free parameters. During the systematic spectral investigation of PCA and HEXTE data for about 50 of the 250 sightings of the source by RXTE, Greiner *et al.* (1998) have noted that even though the composite spectrum consists of 5 different components, the hard component up to 200 keV is best described by a power

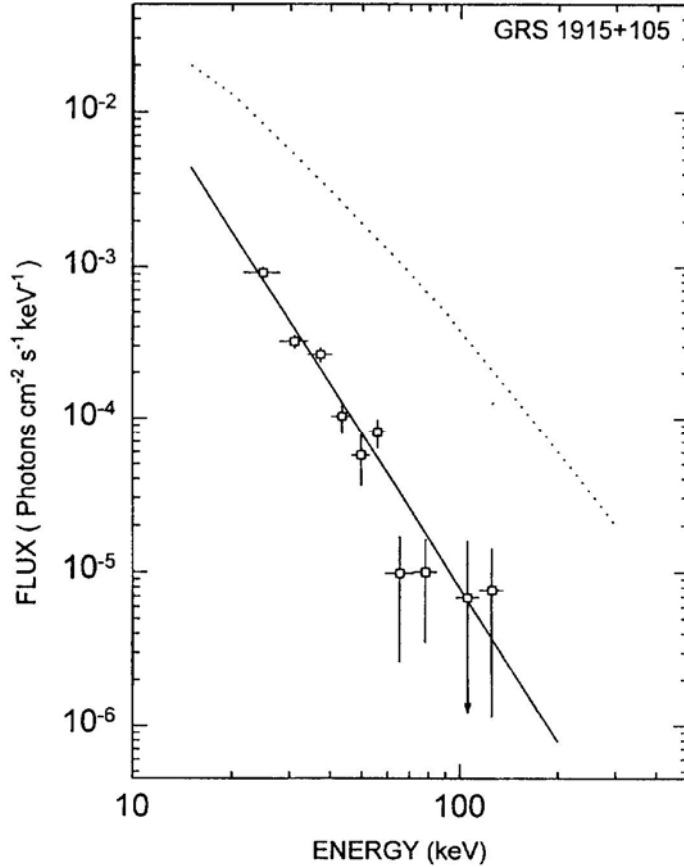


Figure 1. Hard X-ray spectrum of GRS 1915+105. The X-ray spectrum of Cyg X-1 during ‘low hard’ state is shown in dotted line for comparison.

law model. The contribution is always present and is highly varying both in intensity and power index -2.0 and -4.8 .

Surprisingly, the spectral index of 3.34 ± 0.25 measured in the quiescent state compares very well with the spectral measurement from OSSE detector in the 50–300 keV energy band who report an average spectral index of 3.08 ± 0.06 from 3 observations during the peak intensity of 1996 flare (Grove *et al.* 1998). Similarly, Greiner *et al.* (1998) have also reported the best fit power law index $\alpha \sim 3.2$ in the 1–200 keV band for the Oct. 1997 flare.

For the analysis of timing properties of GRS 1915+105, we have searched our data for quasi-periodic oscillations in the 20–140 keV band. The detector counts in two separate sightings were first binned in 0.032 sec intervals and power spectrum analysis was performed using FTOOLS. The summed power density spectrum in the 0.0005–18 Hz are is shown in Fig. 2. It is clearly seen from the figure that data above 0.01 Hz are completely flat. The broad QPO peak visible between 0.025 and 0.045 Hz has a confidence level of only 90%. A low level QPO at 3.4 Hz in the PCA data on March 27th is reported by Trudolyubov *et al.* (1998) however, their data search is restricted to lower time scales. GRS 1915+105 is a peculiar source in which the QPO

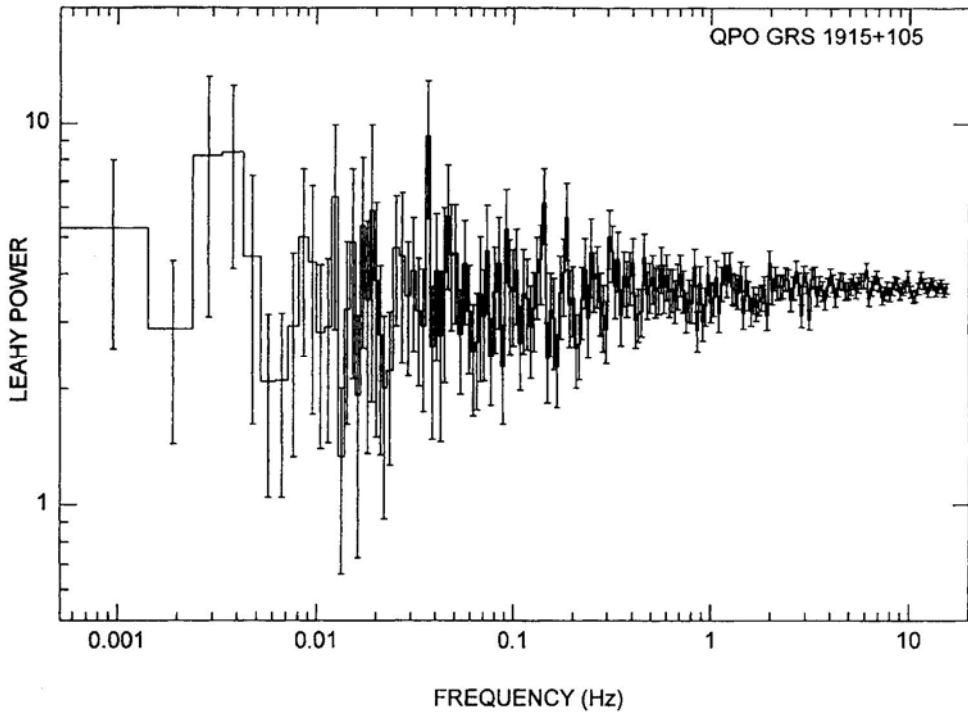


Figure 2. Power density spectrum in the 20-140 keV energy band.

frequency varies continuously in a random fashion. For example, a centroid frequency of 0.003 Hz for QPO was observed on June 16th, 1996 (Morgan *et al.* 1997) while the source was in the flaring mode rather than the featureless low intensity state during the time of present observation. However, from the analysis of the PCA and HEXTE data, Munno *et al.* (1999) find that frequency of the QPO is best correlated to the temperature of the inner accretion region. The presence of very low frequency QPO during the steady quasi-low state is quite probable. The low power for the feature is due to the fact that a correlation between the spectral and temporal states suggest that for power law index $\alpha > 3.05$ source behaves QPO quiet (Markwardt *et al.* 1999).

3.1 Spectral evolution

GRS 1915+105 was in the post-burst low intensity state during the present observations. In figure 3 we have plotted the X-ray light curve of the source taken from the BATSE data. The lowest intensity state corresponding to $0.02 \text{ ph.cm}^{-2} \text{ s}^{-1} \text{ keV}^{-1}$ is shown by the dotted line in the figure and the date for our observations is marked by an arrow. It is seen from the figure that our observation followed a month after the high hard X-ray flux of 0.2 photons recorded by the BATSE detectors and average daily flux on the day was a factor of ~ 3 higher than the lowest flux. The ASM light curve during this period showed a steady behaviour at $\sim 300 \text{ mCrab}$ (20c/s) and is shown in the upper panel in figure 3. It is also seen in the figure that light curves in the soft and hard X-ray band may not be one-to-one correlated at all times.

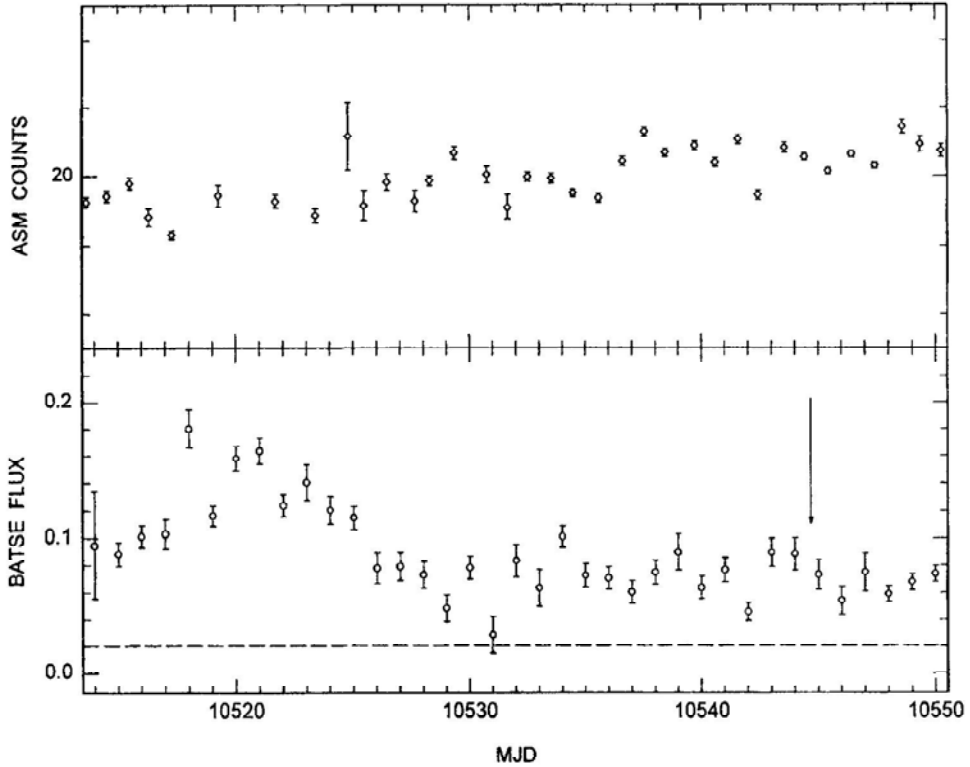


Figure 3. X-ray light curve of GRS 1915+105 in the 20120 keV band from BATSE data. The minimum intensity level is marked by the dotted line and the source intensity level corresponding to present observations is shown by an arrow.

In order to observe the change in the hard X-ray spectrum on a day-to-day basis in the high-to-low transit phase during the post-burst state, we have used the spectral data from PCA and HEXTE before and after our observations. The data are shown in figure 4. The dotted and dashed lines in the figure represent the PCA and HEXTE composite observed flux of the source on February 26th, 1997 and April 2nd, 1997 (Borozdin *et al.* 1999). OSSE data during the 1996 flare (Grove *et al.* 1998) is shown by the solid line in the figure. In terms of integral comparison of low state data shown in figure 4, the measured BATSE flux for the three dates are 0.10, 0.101 and 0.094 $\text{ph.cm}^{-2}\text{s}^{-1}\text{keV}^{-1}$ respectively and the corresponding best fit parameters on hard component from the PCA data give the flux levels to be comparable at 10.12, 10.0 and 11.14 nano-ergs $\text{cm}^{-2}\text{s}^{-1}$ for the three observations.

Three points can be noted from the figure:

- (i) Both the flux levels and the spectral shape on April 2nd (dotted line) observation is in good agreement with our measurements of March 30th.
- (ii) For energies above 20 keV the data for February 26th is higher by a factor about 2 and the corresponding increase during maxima of the flare in 1996 is by a factor ~ 10 .
- (iii) The low energy data below 10 keV does show a crossover.

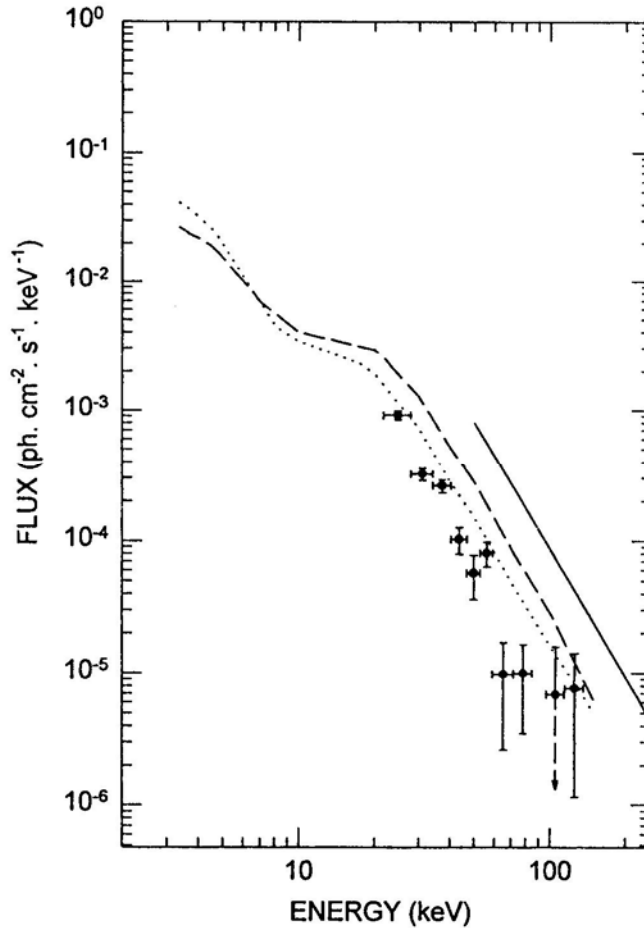


Figure 4. A comparison of the GRS 1915+105 spectra: ● present data, dashed and dotted lines: PCA+HEXTE data on February 9th, 1997 and April 2nd, 1997 and solid line: OSSE data at peak during high state.

In the disk accretion models with advection dominated flow near to the stellar surface, a two temperature plasma is formed at the boundary layer (Narayan, Kato & Honna 1997; Chen, Abramowicz & Lasota 1997) and the hard X-ray and gamma ray emission is believed to originate in the inner region by comptonization of the soft X-ray photons most of which are supplied by the cool outer disk. Considering the comptonization due to bulk motion near to the stellar surface during the high state in black hole binary X-ray source, Ebisawa *et al.* (1996) have proposed, that two distinct spectral indices in the hard X-ray band corresponding to ‘high soft’ and ‘low hard’ state of the source. However, taking by itself the comparison of high energy spectral data above 20 keV during various phases of the source activity as seen in figure 4, clearly suggests that except for increase in the integral emission from the source, the spectral shape does not show any perceptible variation. This is a most significant inference which directly relates to the physical characteristics of the emission mechanism for the non-thermal component. Since the emitted power of

$\sim 2.3 \times 10^{-7}$ erg cm $^{-2}$ s $^{-1}$ from the source in hard X-ray band is substantially higher than the bolometric flux of disk black body component in the low energy band (Greiner *et al.* 1998), the absence of spectral variation during the quiescence and the outburst should be the true indicator of the source properties. Therefore, it follows that during the composite spectral fitting, except for scaling the flux contribution above 20 keV, non-thermal power index should not be made a free parameter. As a result, the spectral properties of the thermal component should be inferred by computing the low energy residuals.

During comptonization, only if $4kT_e > h\nu$ the seed photons will be upgraded in energy and the increase in photon energy on average during each scattering is given by $\frac{\nu'}{\nu} \sim 1 + \frac{4}{3}[\gamma^2 - 1]$, even for a Maxwellian distribution of electrons with $kT_e \ll m_e c^2$. Therefore, multiple scattering even by a Maxwellian gas can lead to very high photon energies. In a non-relativistic plasma where $kT_e \ll m_e c^2$ and $\tau \ll 1$, the average number of scattering for the seed photon $n_{s,2} \sim \tau^2$ and the probability density for multiple scattering is given as; $P(n_s) \propto \exp\left[-\frac{n_s \pi}{3(\tau + \frac{2}{3})^2}\right]$. The emergent spectrum therefore, develops into a unified power law from the ensemble of spectra produced by photons scattered by differing number of times. The emergent spectrum however, will be radically modified in the presence of the seed input spectrum and if the scattering electron cloud has a temperature gradient. Since the high energy photons arise after a large number of scatterings, the direction vector and the origin of the seed photons are completely forgotten. Furthermore, the reflected to transmitted ratio for photons above 15 keV is ~ 1 , the spectral index of the emergent photons is almost independent of the source geometry i.e. whether the seed photons are distributed uniformly in the disk or located on one side of the disk (Pozdnyakov *et al.* 1983). In the limiting case spectral index should become -1.5 for monoenergetic seed photons and Maxwellian distribution of the electron scatterers (Titarchuk *et al.*, 1998). The expected power will be however, reduced in the later case due to integration over limited solid angle.

We can therefore, conclude that the hard X-ray and gamma ray emission in GRS 1915+105, results mainly from the comptonization of soft X-ray photons from the outer disk in the hot boundary layers of the inner disk and thereby giving rise to a power law spectrum independent of the changes in the luminosity level of the source, which in turn is coupled to the level of mass accretion. In the alternate assumption of seed photons coming from the inner disk will lead to changes in the spectrum directly relating to the level of accretion. A single power law fit up to 300 keV for the GRS 1915+105 (Grove *et al.* 1998) is in contrast to the classical BH candidate Cyg X-1, in which the observed spectral index shows steepening above 100keV (Tanaka and Lewin 1995).

3.2 Axiomatic model

The phenomenological arguments about the physical characteristics of GRS 1915+105 suggest the compact object to be a black hole. The X-ray luminosity of the source is measured to be $> 10^{39} \times (D/12.5\text{kpc})^2$ during the violent outburst of the source. Similarly, the presence of dominant QPO during high state resembles the nature of well known BH candidate Cyg X-1. The mass estimates of the black hole however varies between $10M_\odot$ and $33M_\odot$. Assuming that 67 Hz QPO represents the innermost stable orbit of non rotating black hole, the estimated mass of the X-ray source is

$33M_{\odot}$ and if the QPO arises in the g-mode oscillations in the inner disk, the derived mass limit is $10M_{\odot}$ (Nowak *et al.* 1997; Morgan *et al.* 1997). Also, following Manchanda (1999), if the $52d$ period seen in the X-ray light curve represents the orbital period of the binary system, the primary star should have a mass of $\sim 8M_{\odot}$.

Therefore, as a working hypothesis one can assume that the X-ray emission in GRS 1915+105 is due to the compact object accreting mass from its binary companion. However, any scheme proposed for the observed dynamical properties must account for the three well know features:

- (i) Long term temporal nature of random variation between quiescent and flaring episodes,
- (ii) the generation of QPO and their relation with the geometrical variables, and
- (iii) a Power-law hard X-ray spectrum and its non-evolution.

From the detailed analysis of these parameters observed from the PCA and HEXTE data since 1996, a variety of geometrical configurations and the corresponding best fit parameters have been discussed in literature (Belloni *et al.* 1997b; Titarchuk *et al.* 1998a; Titarchuk & Zannias 1998; Laurent & Titarchuk 1998; Narayan *et al.* 1997; Yadav *et al.* 1999). These models mainly consider the accretion on to the black hole as the starting point and the dynamical and thermodynamical details differ in the inner region of the accretion disk.

In the standard model for mass accretion in a binary system the matter falling on to the compact object releases the gravitation potential energy which heats the gas and emits radiation while the transfer of the mass from the primary to the compact object takes place either through the Roche lobe overflow or by the stellar wind (Shakura & Sunyaev 1973; King 1995). Since the accreting gas will have intrinsic angular momentum, a Keplarian disk will be formed around the compact object. The exact spectral behaviour of the emergent photons will be determined by the accretion geometry, dominant heating and cooling mechanism, optical thickness of the gas in the emission region, net heating and cooling rates, radiation pressure, magnetic fields and the boundary conditions at large distance as well as stellar surface. Detailed description of various idealized cases has been discussed in literature (Shapiro & Teukolsky 1983; Abramowicz & Percival 1997; and references therein). In the specific case of accretion on to a black hole compact object, the ultrasoft and the soft X-ray excess in the 2–10 keV energy region is mainly due to the fact that the main cooling mechanism near to the surface of black hole is almost 100% advection (Chen *et al.* 1997a; Narayan & Yi, 1995a, 1995b) and the electron temperature does not rise to very high kT value. The hard X-ray spectrum is believed to originate in the inverse Compton scattering of the low energy photons (Sunyaev & Titarchuk 1985) which further gets modified at lower energies due to the bulk motion of the material close to the black hole (Chakrabarti & Titarchuk 1995). In a hot tenuous plasma bremsstrahlung and recombination losses are small and the energy exchange between electrons and photons is controlled by the multiple scattering. For $4kT_e > h\nu$, the seed photons are upgraded in energy and a composite power law spectrum therefore emerges due to the superposition of the photons scattering by differing number of times. The long term variability and the spectral evolution in such models are coupled to the rate of accretion and the changes in the physical characteristics of emission region.

Even in an oversimplified model, the accreted material must finally rest at the stellar surface at $R_0 = R_{NS}$ or R_{BH} ($= 3R_g$), where R_{NS} , R_{BH} represent the radii of a

neutron star and a black hole and R_g is the Schwarzschild radius. The gas flowing from the Keplerian disk to the surface therefore, must adjust to the new boundary condition thus effecting the thermodynamical properties of the medium. The innermost orbit at which the gas is in Keplerian motion is termed as the centrifugal barrier at $R = R_{CB}$ by Titarchuk *et al.* (1998a) who suggest that super Keplerian flow may occur at this boundary and give rise to the QPO in GRS 1915+105. This hot boundary layer can also generate the hard X-ray photons. It has been also proposed that the flow inside this boundary may be advection driven accretion leading to lower effective heating and low kT value ($\sim 1-2$ keV) thereby leading to the enhanced soft X-ray emission as seen in the BH candidates (Narayan & Yi 1995a; and references therein).

While these models can explain the instantaneous nature of the source, the long term variability of the source from quiescent to outburst phases requires major modification to the accretion flow. The estimated accretion rate for the observed luminosity variation corresponds to $\dot{M} > 2 - 10 \times 10^{-8} M_{\odot}$ for the quiescent phase and a variable enhancement by a factor of ~ 2 during the active phase. Belloni *et al.* (1997a) have proposed the existence of the unstable disk to account for the transient high intensity episodes from the source.

In order to derive new constraints on the mass accretion in GRS 1915+105 we have performed rank analysis of the BATSE daily average source intensity in the 20–100 keV energy band. In our view the hard X-ray flux is the best indicator as it is not affected by the model dependent emission parameters as well as various correction factors due to intervening matter density and the uncertainties of detector response matrix. The data is shown in figure 5. Apart from considerable flaring

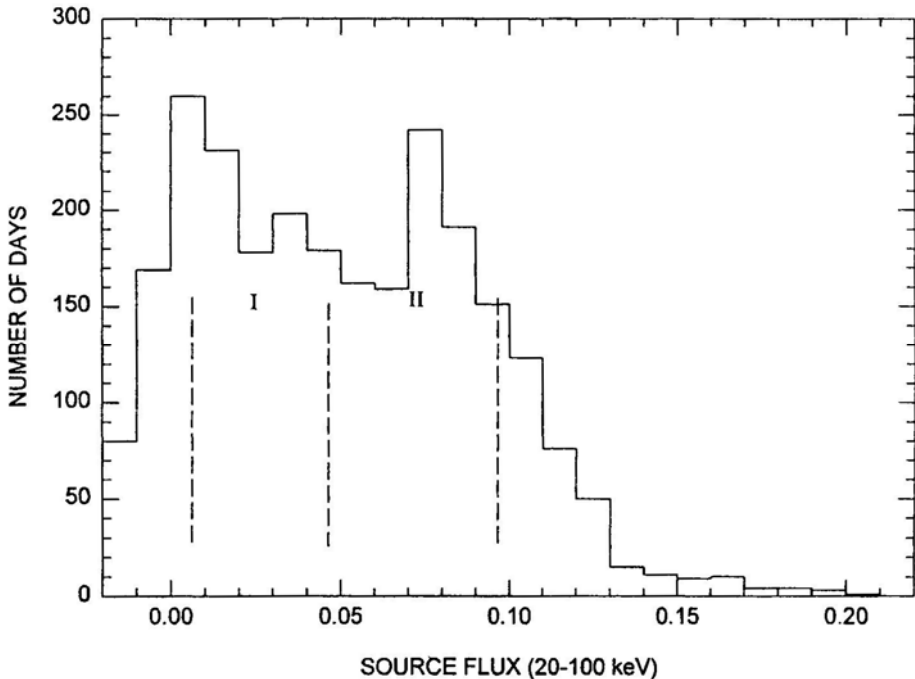


Figure 5. Rank distribution of the measured daily averaged X-ray intensity of GRS 1915+105 in the 20–100 keV band from BATSE data.

activity even above the flux level above $0.12 \text{ ph.cm}^{-2} \text{ s}^{-1} \text{ keV}^{-1}$, two distinct intensity levels marked by the peaks are clearly visible in the figure and are labeled as I and II. An empirical fit with two Gaussian shapes corresponding to the intensity level of $0.015 \text{ ph.cm}^{-2} \text{ s}^{-1} \text{ keV}^{-1}$ and $0.8 \text{ ph.cm}^{-2} \text{ s}^{-1} \text{ keV}^{-1}$ can fairly represent the data. This clearly points to two quasi-steady levels of mass accretion during different phases of source activity. We term the region I as corresponding to the quiescent state during which the source has low luminosity and region II defines the active phase with high luminosity state and caused by an enhanced accretion signifying the change in accretion geometry and during which the flaring activity gets amplified.

In summary, GRS 1915+105 has two quasi-steady luminosity levels signifying different levels of mass accretion and any geometrical model must provide for this change over. It is also seen from the figure that the source spends almost equal amount of time in the two stages of X-ray activity and therefore, the models ascribing this feature to be a simple statistical behaviour of change in accretion, are not tenable. The Gaussian distributions around the mean flux levels may however, arise due to statistical variations in the accreted mass. A two level steady accretion modes of GRS 1915+105 have also been inferred by Munno *et al.* (1999) from the correlation of QPO and the spectral states of the source during the detailed analysis of PCA data. It is found that 0.5–10 Hz QPO serves as a marker for the two modes. In the presence of the QPO, the source spectrum is primarily power-law while the disk emission giving rise to dominant soft X-ray flux is observed when the QPO is absent. Changing levels of accretion in a disk geometry have built in constraints. For example, in the unified model of Belloni *et al.* (1997b), rapid removal and replenishment of the inner parts of the optically thick accretion disk can only take place at viscous time scales. While a detailed look at the X-ray light curve suggests that large changes in luminosity can occur within 2 to 3 minutes. In the following, we outline a new geometrical structure for the inner accretion disk, which can provide the two accretion modes in a natural way.

We hypothesize that inner accretion disks may have a multiple ring structure with the first node touching the stellar surface through which actual mass is accreted on to the compact object. The schematic for the geometrical structure is shown in figure 6.

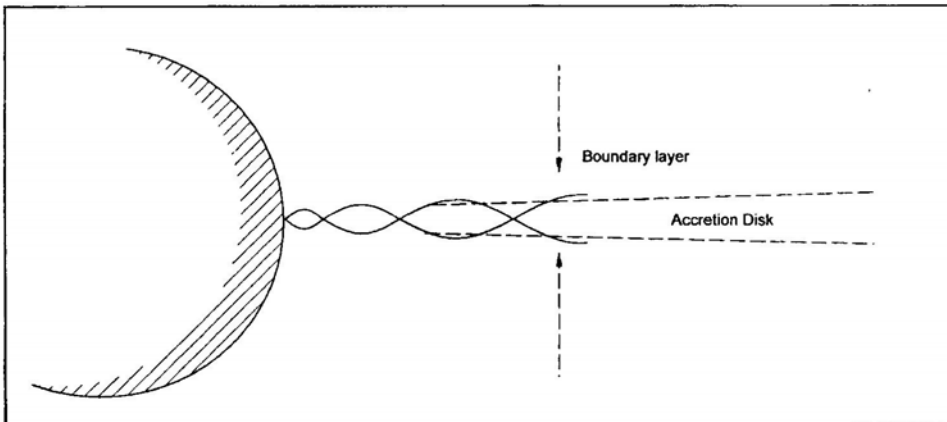


Figure 6. Geometrical structure of the inner accretion disk of GRS 1915+105.

An apparent correlation between the quiescent time and the burst duration during the fast flickering phase of the source does suggest a discrete annular behaviour of the inner disk accretion. Similarly, Titarchuck *et al.* (1998a) have also argued that QPO may arise due to non radial oscillations caused by the formation of kinks and shocks in the super Keplerian flow. Existence of the acoustic waves in the hot plasma have also been proposed as the possible source for QPO emission (Chen *et al.* 1997a).

The global solutions of the ADAF flow for various models of disk parameters (α, \dot{M} , Pressure, Mack number) suggest that a transonic region is set up in the boundary layer of inner and outer disk at $r \sim 10^3 r_s$ (Chen *et al.* 1997b). We therefore, propose that during the dynamical adjustment from the boundary of the Keplerian disk to the stellar surface, transverse oscillations are excited at the boundary and propagate inward with decreasing amplitude. Added to this the existence of inherent p and g mode oscillation of the disk (Nowak & Wagner 1993), and progressively decreasing micro turbulence from the boundary layers to the stellar surface, a ring structure may be formed in the inner part. The reflected shock generated by the land-fall on to the stellar boundary, should further help stabilize the ring geometry. In the equilibrium conditions during the quiescent phase the mass accretion on to the surface in this geometry is controlled by the nodal cross-section. A bi-modal mass accretion as inferred earlier and consequent increased luminosity in our model arises when above a specific accretion rate, the node is pushed into the stellar boundary, and the available cross-section for mass transfer is increased. This can be triggered by a change in the accretion rate from the companion star into the boundary layers giving rise to enhanced turbulence. Such a change over appears natural as the Reynolds number of the accretion flow is proportional to the accretion rate and is believed to be the determining factor for the QPO frequency in the source. Fluctuations in the mean accretion rate may arise due to geometrical changes leading to oscillations of the inner most ring caused by the difference in the incoming and outgoing material. We believe that such ordered structure is much more likely than the formation of discontinuities which are hypothesized to remove the angular momentum from the accreted material and a continuously varying size of vacuum ring around the source hypothesized by Belloni *et al.* (1997b) to explain the observation of burst duration-to quiescent time correlation.

This simple empirical model predicts two observable features. First, the high-low transitions can take place much faster than the viscous time scale t_{vis} given by; $t_{vis} = 30 \left(\frac{\alpha}{0.01}\right)^{-1} R_7^{7/2} \dot{M}_{18}^{-2} \geq 3000 \text{sec}$, for best fit parameters of the accretion disk up to the transonic boundary. Second, for an equivalent luminosity level, the spectral parameters are independent of rapidity at which the high-low transition takes place.

The difference between the emission behaviour of GRS 1915+105 and the classical black hole Cyg X-1 can be understood in terms of its transient nature. In the currently accepted models, the transient sources are high mass X-ray binaries (HMXB) with generally a Be star companion, which provides the accretion material through mass ejection episodes. In fact all the 17 transient sources discovered so far, are associated with such systems (Paradisj van 1995). Even though in most of the transient sources, the compact object is a pulsating neutron star, the occurrence of Be star black hole binary system is not excluded by any selection rule. Since the mass ejection rate from Be star can be not only large but highly variable and thus can account for the luminosity transitions seen in GRS 1915+105. In comparison, the

optical companion of Cyg X-1 is a O type star, which as a class can give large winds but do not show large changes in the mass-loss rate. It is surmised that large variations in the mass transfer rate from the Be star above the Eddington limit results in the different geometrical structures for the inner accretion disk in GRS 1915+105 as discussed earlier.

Acknowledgement

I wish to thank Prof. A. R. Rao and Dr. J. S. Yadav for their comments on the manuscript and the RXTE and the BATSE teams for making the data available on public archives.

References

- Abramowicz, M. A., Percival, M. J. 1997, *Class. Quantum Grav.*, **14**, 2003.
- Belloni, T., Mendez, M., King, A. R., Van der Kliss M., van Paradisj, J. 1997a, *Astrophys. J.*, **479**, L 145.
- Belloni, T., Mendez, M., King, A. R., Van der Kliss, M., van Paradisj, J. 1997b, *Astrophys. J.*, **488**, L 109.
- Borozdin *et al.* 1999, *Astrophys. J.*, **517**, 367.
- Castro-Tirado, A. J., Brandt, S., Lund, N. 1992, *IAU Circ.* **5590**.
- Chakrabarti, S., Titarchuck, L. 1995, *Astrophys. J.*, **455**, 623.
- Chen, X., Swank, J. H., Tamm, R. E. 1997, *Astrophys. J.*, **477**, L41.
- Chen, X., Abramowicz, M. A., Lasota, J. 1997, *Astrophys. J.*, **485**, L75.
- D' Silva, J. A. R., Madhwani, P. P., Tembhurne, N., Manchanda, R. K. 1998, *Nucl Instr. And Meth.*, **A412**, 342.
- Ebisawa, K., Titarchuck, L., Chakrabarti, S. 1996, *PAS J*, **48**, 59.
- Eikenberry, S. S. *et al.* 1998, *Astrophys. J.*, **494**, L 61.
- Fender, R. P. *et al.* 1997, *Mon. Not. R. astr. Soc.*, **286**, 629.
- Foster R. S. *et al.* 1996, *Astrophys. J.*, **467**, L81.
- Greiner, J., Morgan, E. H., Remillard, R. 1996, *Astrophys. J.*, **473**, L107.
- Greiner, J., Morgan, E. H., Remillard, R. 1998, preprint, Astro-ph/9806323.
- Grove, J. E., Johnson, W. N., Kroeger, R. A., McNaron-Brown, K., Skibo, J. G.: 1998, *Astrophys. J.*, **500**, 898.
- King, A. 1995 in *X-ray Binaries*, (ed.) Lewin, Paradisj & van den Heuvel (Cambridge. Univ. Press), 410.
- Laurent, P., Titarchuck, L. 1998, Preprint astro-ph/9808015.
- Manchanda, R. K. 1999, Preprint.
- Markwardt, C. B., Swank, J. H., Taam, R. E. 1999, *Astrophys. J.*, **513**, L37.
- Mirabel, I. F., Rodriguez, L. F. 1994, *Nature*, **46**.
- Mirabel, I F. *etal.* 1994, *Astr. Astrophys.*, **282**, L17.
- Morgan, E. H., Remillard, R. A., Greiner, J. 1997, *Astrophys. J.*, **482**, 993.
- Munno, M. P., Morgan, E. H., Remillard, R. A. 1999, Preprint, Astro-Ph 9904087.
- Narayan, R., Kato, S., Honma, F. 1997, *Astrophys. J.*, **476**, 49.
- Narayan, R, Yi, I. 1995a, *Astrophys. J.*, **444**, 213.
- Narayan, R, Yi, I. 1995b, *Astrophys. J.*, **452**, 710.
- Nowak, M. A. *et al.* 1997, *Astrophys. J.*, **477**, L91.
- Nowak, M. A., Wagner, R. V. 1993, *Astrophys. J.*, **418**, 187.
- Pozdnyakov, L. A., Sobol, I. M., Sunyaev, R. A. 1983, *Sp. Sci. Rev.*, **2**, 189.
- Paradisj Jan, V. 1995, in *X-ray Binaries*, (ed.) Lewin, Paradisj & van den Heuvel (Cambridge Univ. Press), 537.
- Shakura, N. I., Sunyaev, R. A. 1973, *Astr. Astrophys.*, **24**, 337.

- Shapiro, S. L., Teukolsky, 1983, in *Black holes, white dwarfs and Neutron stars*, (John Wiley & Sons Publ.)
- Sunyaev, R. A., Titarchuck, L. G. 1985, *Astr. Astrophys.*, **143**, 374.
- Tanaka, Y., Lewin, W. H. G. 1995, in *X-ray Binaries*, (ed.) Lewin, Paradijs & van den Heuvel (Cambridge Univ. Press), 126.
- Trudolyubov, S., Churazov, E., Gilfanov, M. 1998, preprint ASTR-Oph/9811449.
- Titarchuck, L., Lapidus, I., Muslimov, A. 1998, *Astrophys. J.*, **499**, 315.
- Titarchuck, L., Zannias, T. 1998, *Astrophys. J.*, **493**, 863.
- Yadav, J. S. *et al.* 1999, *Astrophys. J.*, (in press).